electronics

MDPI

Communication

Optimized Polarization Encoder with High Extinction Ratio for Quantum Key Distribution System

Pengcheng Wang [1,2], Qianqian Zhang [3], Huanwen Xie [3] and Banghong Guo [1,2,*]

[1] Guangdong Provincial Key Laboratory of Nanophotonic Functional Materials and Devices, South China Normal University, Guangzhou 510006, China
[2] Guangdong Provincial Key Laboratory of Quantum Engineering and Quantum Materials, South China Normal University, Guangzhou 510006, China
[3] National Quantum Communication (Guangdong) Co., Ltd., Guangzhou 510535, China
* Correspondence: guobh@scnu.edu.cn

Abstract: Polarization encoding is a promising approach for practical quantum key distribution (QKD) systems due to its simple encoding and decoding methodology. In this study, we propose a self-compensating polarization encoder (SCPE) based on a phase modulator, which can be composed of commercial off-the-shelf (COT) devices. We conducted a proof-of-concept experiment to test the SCPE, which demonstrated an in-system quantum bit error rate (QBER) of 0.53% and long-term running stability without any active adjustments. Additionally, we conducted experiments with transmission over commercial fiber spools of lengths up to 100 km and obtained a secure finite key rate of 3 kbps. Our polarization encoder is a promising solution for various polarization encoding protocols, including BB84, MDI, and RFI.

Keywords: quantum key distribution; polarization encoder; Sagnac loop

check for updates

Citation: Wang, P.; Zhang, Q.; Xie, H.; Guo, B. Optimized Polarization Encoder with High Extinction Ratio for Quantum Key Distribution System. *Electronics* **2023**, *12*, 1859. https://doi.org/10.3390/electronics12081859

Academic Editors: He-Liang Huang, Chu Guo, Zu-En Su and Shi-Lei Su

Received: 20 March 2023
Revised: 1 April 2023
Accepted: 4 April 2023
Published: 14 April 2023

Copyright: © 2023 by the authors. Licensee MDPI, Basel, Switzerland. This article is an open access article distributed under the terms and conditions of the Creative Commons Attribution (CC BY) license (https://creativecommons.org/licenses/by/4.0/).

1. Introduction

Quantum key distribution (QKD) can realize secure key sharing and solve the problem of key distribution in information security [1,2]. Thanks to Heisenberg's uncertainty principle and the quantum no-cloning theorem, any disturbance introduced by eavesdropping inevitably leads to a higher-than-expected quantum bit error rate (QBER) [3]. Since the first QKD protocol, named BB84 protocol, was proposed by Bennett and Brassard in 1984 [4], numerous QKD protocols have been developed based on entangled photon pairs [5,6], continuous variables [7–9], and discrete variables [10–15]. The feasibility of these protocols have been experimentally verified in optical fiber [9,12], underwater channels [16], and free-space [17,18]. In practical QKD experiments, phase coding and polarization coding are commonly utilized. For polarization-encoded QKD systems, some researchers use four independent lasers to generate photons with four different polarization states [17,19,20]. However, this method is susceptible to side-channel attacks by eavesdroppers, as different lasers may have varying characteristics, such as frequency and emission time [21]. To ensure the indistinguishability of light pulses with different polarization states, some researchers have chosen to use a single laser and implement polarization encoding through active polarization modulators [22–24]. Unfortunately, active polarization modulators require high-voltage pulses to drive them, which are highly sensitive to external environmental influences and have low modulation rates. Researchers have introduced phase-modulation polarization encoding in a polarization-encoded QKD system because polarization coding essentially involves differential phase coding between two orthogonal polarization states.The Mach–Zehnder (MZ) interferometer scheme [25–27] and the Sagnac scheme [28–32] have been proposed. The MZ interferometer scheme is difficult to maintain stability, whereas the Sagnac scheme has high intrinsic stability and encodes the four polarization states of $|L\rangle$, $|R\rangle$, $|D\rangle$, $|A\rangle$. However, many polarization coding schemes currently

use polarizing beam splitters (PBS) for decoding, meaning they require an additional step to transform the polarization states from $|L\rangle, |R\rangle, |D\rangle, |A\rangle$ to $|H\rangle, |V\rangle, |D\rangle, |A\rangle$. An additional polarization converter to transform the polarization states into $|H\rangle, |V\rangle, |D\rangle, |A\rangle$ will increase the complexity of the QKD system. It is evident that the Sagnac scheme must work together with the corresponding decoder and cannot serve as a substitute for the polarization modulator.

In this paper, we propose a self-compensating polarization encoder (SCPE) named SCPE, which exhibits high intrinsic stability and is insensitive to the phase differences caused by temperature changes. Furthermore, the SCPE has a high extinction ratio and low bit error rate. Importantly, the SCPE can directly generate the four polarization states of $|H\rangle, |V\rangle, |D\rangle, |A\rangle$, effectively replacing the need for polarization modulators in QKD systems. In experimental tests, the SCPE exhibited an average quantum bit error rate (QBER) of 0.53% without any active compensation. The QKD system was also tested over commercial optical fibers, where a total of $N = 10^{10}$ pulses were sent out, and we ultimately achieved a key rate of 3 kbps at a distance of 100 km.

2. Materials and Methods

The SCPE is shown in Figure 1, with horizontal light pulses coming in from the laser diode, and the polarization controller (PC) can transform the horizontal polarized light into a superposition of horizontal and vertical polarization. We adjusted the transmission matrix of PC as

$$\begin{pmatrix} 1 & i \\ i & 1 \end{pmatrix}$$

Thus, the polarization state arriving at the PBS1 can be described as

$$\begin{pmatrix} 1 \\ i \end{pmatrix}$$

PBS1 marks the beginning of the Sagnac interferometer, which consists of a polarization beam splitter (PBS), a phase modulator (PM), and a Faraday rotator (FR). The interferometer utilizes a PBS1 to separate the horizontally and vertically polarized parts. The vertically polarized part travels in the clockwise direction (CW), whereas the horizontally polarized part travels in the counterclockwise direction (CCW). The horizontally polarized part propagates in the CCW direction and encounters a PM, where a phase of φ is applied to it. After passing through the PM, the horizontally polarized part encounters the Faraday rotator, which rotates its polarization state by 90°. This causes the horizontally polarized part to exit the Sagnac interferometer in a vertically polarized state. In the CW direction, the vertically polarized part encounters the Faraday rotator, which first rotates its polarization state by 90°. The next component encountered is a PM that does not apply any phase to the part propagating in the CW direction. As a result, the vertically polarized impinges once again on the PBS1, exiting the Sagnac interferometer in a horizontal polarized state. As the length of the fiber optic traversed is the same for both CW and CCW pulses, it ensures that they exit the Sagnac interferometer simultaneously, resulting in the perfect recombination of the two orthogonal polarization states at the PBS1. The emerging polarization state is combined at PBS1, as given by

$$\begin{pmatrix} i \\ e^{i\varphi} \end{pmatrix}$$

The combined beam out of the PBS1 and passes though the PC can be described as

$$\begin{pmatrix} 1 & i \\ i & 1 \end{pmatrix} \begin{pmatrix} i \\ e^{i\varphi} \end{pmatrix} = \begin{pmatrix} i + ie^{i\varphi} \\ e^{i\varphi} - 1 \end{pmatrix} \quad (1)$$

To achieve output polarization states of $|H\rangle$, $|V\rangle$, $|D\rangle$, and $|A\rangle$, we load modulation voltages of 0, $V_{\frac{\pi}{2}}$, V_{π}, and $V_{\frac{3\pi}{2}}$ on the CCW pulses, while the CW pulses arrive without any modulation signal.

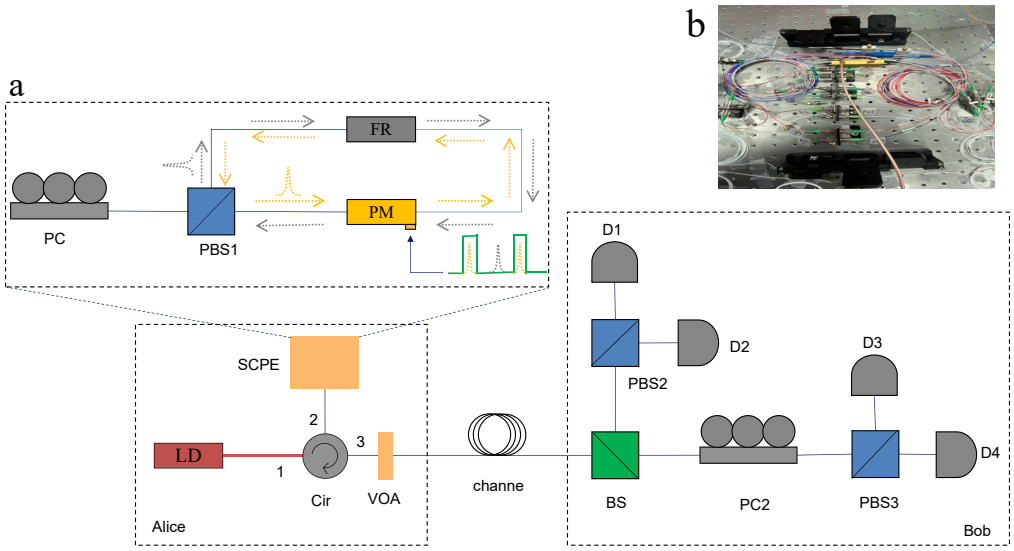


Figure 1. Schematic and experimental diagram of the QKD system. (**a**) Schematic diagram of SCPE LD, laser diode (Qasky Co. Ltd., Wuhu, China); Circ, circulators; PC, polarization controller; PBS, polarized beam splitter; PM, phase modulator (China Electronics Technology Group Co. Ltd., Chongqing, China); FR, Faraday rotator; VOA, variable optical attenuator; D1–D4, single-photon detector (Langyan Optoelectronic Technology Co. Ltd., Shanghai, China). (**b**) Experimental setup of the QKD system.

In detail, if 0 voltage is applied to the CCW, the polarization state becomes

$$\left|\psi_{out}^{0}\right\rangle = |H\rangle = 2i\begin{pmatrix}1\\0\end{pmatrix} \tag{2}$$

If $V_{\frac{\pi}{2}}$ voltage is applied to the CCW, the polarization state becomes

$$\left|\psi_{out}^{\frac{\pi}{2}}\right\rangle = |A\rangle = (1-i)\begin{pmatrix}1\\-1\end{pmatrix} \tag{3}$$

If V_{π} voltage is applied to the CCW, the polarization state becomes

$$|\psi_{out}^{\pi}\rangle = |V\rangle = i\begin{pmatrix}0\\1\end{pmatrix} \tag{4}$$

If $V_{\frac{3\pi}{2}}$ voltage is applied to the CCW, the polarization state becomes

$$\left|\psi_{out}^{\frac{3\pi}{2}}\right\rangle = |D\rangle = (-1-i)\begin{pmatrix}1\\1\end{pmatrix} \tag{5}$$

Therefore, the SCPE can generate four polarization states $|H\rangle, |V\rangle, |D\rangle, |A\rangle$ by loading different voltages. To evaluate the performance of the SCPE, we conducted a proof-of-principle experiment using the setup illustrated in Figure 1. The experimental setup is composed of three main parts: the emitter (Alice), the channel, and the receiver (Bob). The transmitter utilizes a semiconductor laser (LD) to generate phase-randomized pulses with a pulse width of 200 ps and a repetition rate of 50 MHz. The laser pulse enters the optical circulator (CIRC) through port 1 and exits through port 2. Subsequently, the laser pulse is introduced into the SCPE. The SCPE modulates the light pulse with the voltage applied by Alice, and the modulated pulse is output from port 3. Afterwards, the pulse passes through an attenuator, where it is attenuated to the single-photon level. Finally, the light pulse is transmitted through the fiber channel to the receiver, which consists of BS, PBS2, PBS3, PC2, and four InGaAs single-photon detectors with a detection efficiency of approximately 10%, a dark count rate of approximately 250 Hz, and gate width of 2 ns. PBS2 assists us in

measuring the states of $|H\rangle$ and $|V\rangle$, while PBS3 and PC2 enable us to measure the states of $|D\rangle$ and $|A\rangle$.

The radio frequency (RF) signal employed for modulation is produced by a signal generator that offers the flexibility to arbitrarily adjust the delay with a precision of 100 picoseconds. The QBERs for Z-base ($|H\rangle$ and $|V\rangle$) and X-base ($|D\rangle$ and $|A\rangle$) were measured for 30 consecutive minutes, as shown in Figure 2. The experimental setup was placed on an optical platform without any additional temperature control during the experiment. The QBER is calculated using [33]

$$QBER = e_0 Y_0 + e_{\text{det}}(1 - e^{-\eta\mu}) \tag{6}$$

where e_{det} is the probability that a photon hit the erroneous detector, η represents the transmittance of the system, and μ is the strength of signal state. Y_0 encompasses the detector's dark count as well as other sources of background, such as stray light emitted from timing pulses. The error rate of the background is $e_0 = \frac{1}{2}$.

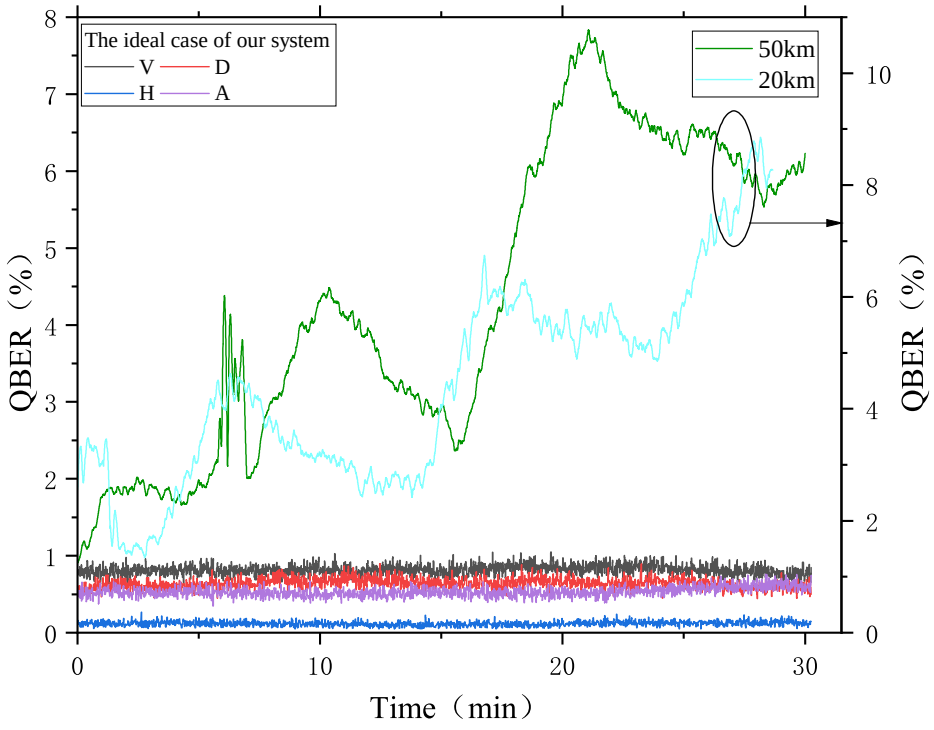


Figure 2. Measured QBERs of four polarization states of $|H\rangle, |V\rangle, |D\rangle, |A\rangle$, and 20 km and 50 km commercial optical fiber for 30 min, demonstrating stability.

As shown in Figure 2, the QBER was found to be 0.1% for H, 0.8% for V, 0.6% for D, and 0.5% for A. The average QBER was 0.53%. The extinction ratio of 29.21 dB was achieved, calculated as the ratio of the maximum number of counts to the minimum number of counts. These measurements demonstrate the high stability and high extinction ratio of the SCPE. Furthermore, QBER was tested for distances of 20 and 50 km for 30 min. The results showed that during 20 min, the QBER remained below 8% at 50 km and 7% at 20 km. After 20 min, the qubit compensation scheme can be applied without the need for additional optical components [34]. To evaluate the secret key rate (SKR) at varying distances, we performed QKD experiments on commercial fibers with lengths of 20 km, 50 km, 70 km, and 100 km, corresponding to measured channel losses of 4.74 dB, 12.05 dB, 17.62 dB, and 22.12 dB, respectively. The typical loss for commercial optical fibers is 0.2 dB/km @ 1550 nm; therefore, the high loss in our fibers may be caused by imperfect

fusion splicing. A two-decoy-state procedure was used to simulate the performance of SKR. The SKR [33]

$$R \geq q\{-Q_\mu f(E_\mu)\, H_2(E_\mu) + Q_1^{L,\nu_1,\nu_2}[1 - H_2(e_1^{U,\nu_1,\nu_2})]\} \quad (7)$$

q denotes the communication efficiency of the BB84 protocol, Q_μ indicates the count rate of the signal state, f(x) is a two-way error correction function, $H_2(x)$ is the Shannon entropy function E_μ denoting the QBER of the signal state, and Q_1^{L,ν_1,ν_2} denotes the lower bound on the count rate of a single-photon pulse in the indicated signal state. e_1^{U,ν_1,ν_2} denotes the upper bound on the QBER of a single-photon pulse in the signal state.

3. Results

We simulated the relationship between secure key rate and distance using the two-decoy-state method and found that our QKD system can achieve a maximum communication distance of 150 km (see Figure 3). Across each distance, a total of $N = 10^{10}$ pulses is sent out. The intensities of the signal light is set to $\mu = 0.56$, and decoy states are simulated as $\nu_1 = 0.23$ and $\nu_2 = 0$. We achieved a secret key rate of 3 kbps at 100 km in experiments (see Figure 3). We compared the secure key rates of Peng [35], Ma [32], and our OKD scheme and found that our QKD scheme has a clear advantage in terms of key rate. To achieve a secure key rate of Mbps, the frequency of the light source should be increased to 1.25 GHz, and an SNSPD with a free-running dark count rate of 500 Hz and a quantum efficiency of 85% should be used. With these parameters, a secure key rate of 12 Mbps can be achieved at a distance of 50 km.

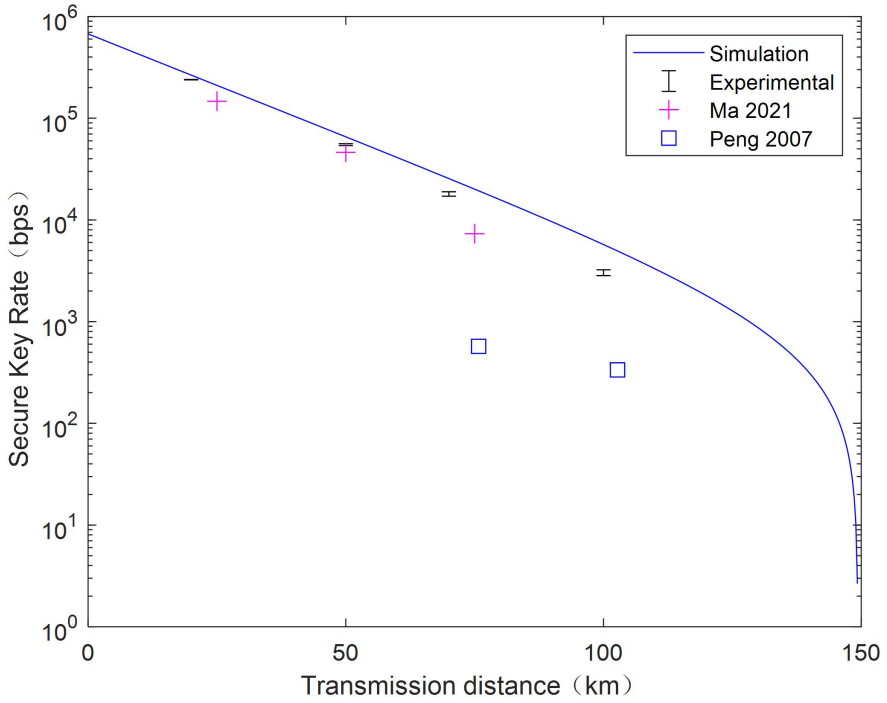


Figure 3. The key rate performance of SCPE. The experimental rate distance performance of SCPE, compared with the theoretical simulations, along with Peng [35] and Ma [32].

Our SCPE produces four linear polarization states of $|H\rangle, |V\rangle, |D\rangle, |A\rangle$, instead of $|L\rangle, |R\rangle, |D\rangle, |A\rangle$, simplifying the QKD system. Additionally, most Sagnac polarization modulators require custom devices, while our improved SCPE can be constructed using only commercially available off-the-shelf (COT) devices, reducing cost and increasing convenience. Table 1 provides a detailed comparison of the performance of our QKD system with other QKD systems.

Table 1. Comparison of polarization coding QKD.

Programs	COT	Average QBER	Distance
TANG [27]	YES	-	-
Costantino [29]	YES	1.23%	-
Yang Li [31]	NO	0.27%	-
Marco [28]	NO	0.2%	-
Di Ma [32]	NO	1%	75 km
OUR	YES	0.53% (see Figure 3)	100 km

4. Conclusions

In conclusion, we have proposed an SCPE, a high-extinction-ratio polarization encoder based on a phase modulator inside a Sagnac interferometer. The stability and feasibility of the SCPE have been directly demonstrated through experimental testing. We also conducted tests on the QBER and secure key of the SCPE. In a laboratory environment, we conducted tests using commercial optical fibers of different communication lengths. A total of $N = 10^{10}$ pulses was sent out for each distance, and we ultimately achieved a secure key rate of 3 kbps at 100 km when the repetition rate of the light source was 50 MHz. Finally, we simulated a secure key rate across a finite key regime and found that our QKD system can achieve a maximum communication distance of 150 km. The highly applicable SCPE utilizes existing commercially available devices, making it a cost-effective solution for metro quantum communication.

Author Contributions: Conceptualization, P.W.; methodology, P.W. and Q.Z.; software, P.W.; validation, P.W. and Q.Z.; formal analysis, P.W.; investigation, P.W. and Q.Z.; writing—original draft preparation, P.W.; writing—review and editing, P.W. and B.G.; visualization, P.W.; supervision, H.X. and B.G.; funding acquisition, B.G. All authors have read and agreed to the published version of the manuscript.

Funding: This research was funded by the Key-Area Research and Development Program of Guangdong Province (Grant No. 2018B030325002).

Institutional Review Board Statement: Not applicable.

Informed Consent Statement: Not applicable.

Data Availability Statement: Not applicable.

Acknowledgments: Thanks for the funding from Xijiang Talent and Guangdong Province Doctoral Workstation.

Conflicts of Interest: The authors declare no conflict of interest.

References

1. Wang, X.-B. Beating the Photon-Number-Splitting Attack in Practical Quantum Cryptography. *Phys. Rev. Lett.* **2005**, *94*, 230503. [CrossRef] [PubMed]
2. Pan, Y.; Wang, H.; Shao, Y.; Pi, Y.; Li, Y.; Liu, B.; Huang, W.; Xu, B. Experimental demonstration of high-rate discrete-modulated continuous-variable quantum key distribution system. *Opt. Lett.* **2022**, *47*, 3307. [CrossRef] [PubMed]
3. Chen, Z.-B.; Zhang, Q.; Bao, X.-H.; Schmiedmayer, J.; Pan, J.-W. Deterministic and efficient quantum cryptography based on Bell's theorem. *Phys. Rev. A* **2006**, *73*, 050302. [CrossRef]
4. Bennett, C.H.; Brassard, G. Quantum cryptography. *Theor. Comput. Sci.* **2014**, *560*, 7. [CrossRef]
5. Ekert, A.K. Quantum cryptography based on Bell's theorem. *Phys. Rev. Lett.* **1991**, *67*, 661. [CrossRef]
6. Tittel, W.; Brendel, J.; Zbinden, H.; Gisin, N. Quantum cryptography using entangled photons in energy-time Bell states. *Phys. Rev. Lett.* **2000**, *84*, 4737. [CrossRef]
7. Ralph, T.C. Continuous variable quantum cryptography. *Phys. Rev. A* **1999**, *61*, 010303. [CrossRef]
8. Huang, P.; Wang, T.; Chen, R.; Wang, P.; Zhou, Y.; Zeng, G. Experimental continuous-variable quantum key distribution using a thermal source. *New J. Phys.* **2021**, *23*, 113028. [CrossRef]
9. Ralph, T.C. Security of continuous-variable quantum cryptography. *Phys. Rev. A* **2000**, *62*, 062306. [CrossRef]

10. Yin, H.-L.; Chen, T.-Y.; Yu, Z.-W.; Liu, H.; You, L.-X.; Zhou, Y.-H.; Chen, S.-Y.; Mao, Y.; Huang, M.-Q.; Zhang, W.-J.; et al. Measurement-device-independent quantum key distribution over a 404 km optical fiber. *Phys. Rev. Lett.* **2016**, *117*, 190501. [CrossRef]
11. Boaron, A.; Boso, G.; Rusca, D.; Vulliez, C.; Autebert, C.; Caloz, M.; Perrenoud, M.; Gras, G.; Bussières, F.; Li, M.-J.; et al. Secure quantum key distribution over 421 km of optical fiber. *Phys. Rev. Lett.* **2018**, *121*, 190502. [CrossRef]
12. Yuan, Z.; Plews, A.; Takahashi, R.; Doi, K.; Tam, W.; Sharpe, A.W.; Dixon, A.R.; Lavelle, E.; Dynes, J.F.; Murakami, A.; et al. 10-Mb/s Quantum Key Distribution. *J. Light. Technol.* **2018**, *36*, 3427. [CrossRef]
13. Wang, S.; Chen, W.; Guo, J.-F.; Yin, Z.-Q.; Li, H.-W.; Zhou, Z.; Guo, G.-C.; Han, Z.-F. 2 GHz clock quantum key distribution over 260 km of standard telecom fiber. *Opt. Lett.* **2012**, *37*, 1008. [CrossRef]
14. Zhu, M.; Hu, M.; Guo, B. Free-Space QKD with Modulating Retroreflectors Based on the B92 Protocol. *Entropy* **2022**, *24*, 204. [CrossRef] [PubMed]
15. Hua, X.; Hu, M.; Guo, B. Multi-User Measurement-Device-Independent Quantum Key Distribution Based on GHZ Entangled State. *Entropy* **2022**, *24*, 841. [CrossRef]
16. Hu, C.-Q.; Yan, Z.-Q.; Gao, J.; Jiao, Z.-Q.; Li, Z.-M.; Shen, W.-G.; Chen, Y.; Ren, R.-J.; Qiao, L.-F.; Yang, A.-L.; et al. Transmission of photonic polarization states through 55-m water: towards air-to-sea quantum communication. *Photonics Res.* **2019**, *7*, A40. [CrossRef]
17. Hughes, R.J.; Nordholt, J.E.; Derkacs, D.; Peterson, C.G. Practical free-space quantum key distribution over 10 km in daylight and at night. *New J. Phys.* **2002**, *1*, 43. [CrossRef]
18. Zhang, M.; Huang, P.; Wang, P.; Wei, S.; Zeng, G. Experimental free-space continuous-variable quantum key distribution with thermal source. *Opt. Lett.* **2023**, *48*, 1184. [CrossRef]
19. Bacco, D.; Canale, M.; Laurenti, N.; Vallone, G.; Villoresi, P. Experimental quantum key distribution with finite-key security analysis for noisy channels. *Nat. Commun.* **2013**, *4*, 1. [CrossRef]
20. Vest, G.; Rau, M.; Fuchs, L.; Corrielli, G.; Weier, H.; Nauerth, S.; Crespi, A.; Osellame, R.; Weinfurter, H. Design and Evaluation of a Handheld Quantum Key Distribution Sender module. *IEEE J. Sel. Top. Quantum Electron.* **2015**, *21*, 131. [CrossRef]
21. Nauerth, S.; Fürst, M.; Schmitt-Manderbach, T.; Weier, H.; Weinfurter, H. Information leakage via side channels in freespace BB84 quantum cryptography. *New J. Phys.* **2009**, *11*, 065001. [CrossRef]
22. Kim, Y.-S.; Jeong, Y.-C.; Kim, Y.-H. Implementation of polarization-coded free-space BB84 quantum key distribution. *Laser Phys.* **2008**, *18*, 810. [CrossRef]
23. Grünenfelder, F.; Boaron, A.; Rusca, D.; Martin, A.; Zbinden, H. Simple and high-speed polarization-based QKD. *Appl. Phys. Lett.* **2018**, *112*, 051108. [CrossRef]
24. Jofre, M.; Gardelein, A.; Anzolin, G.; Molina-Terriza, G.; Torres, J.P.; Mitchell, M.W.; Pruneri, V. 100 MHz amplitude and polarization modulated optical source for free-space quantum key distribution at 850 nm. *J. Light. Technol.* **2010**, *28*, 2572–2578. [CrossRef]
25. Yan, Z.; Meyer-Scott, E.; Bourgoin, J.-P.; Higgins, B.L.; Gigov, N.; MacDonald, A.; Hubel, H.; Jennewein, T. Novel High-Speed Polarization Source for Decoy-State BB84 Quantum Key Distribution Over Free Space and Satellite Links. *J. Light. Technol.* **2013**, *31*, 1399. [CrossRef]
26. Pugh, C.J.; Kaiser, S.; Bourgoin, J.-P.; Jin, J.; Sultana, N.; Agne, S.; Anisimova, E.; Makarov, V.; Choi, E.; Higgins, B.L.; et al. Airborne demonstration of a quantum key distribution receiver payload. *Quantum Sci. Technol.* **2017**, *2*, 024009. [CrossRef]
27. Liu, X.; Liao, C.; Mi, J.; Wang, J.; Liu, S. Intrinsically stable phase-modulated polarization encoding system for quantum key distribution. *Phys. Lett. A* **2008**, *373*, 54. [CrossRef]
28. Avesani, M.; Agnesi, C.; Stanco, A.; Vallone, G.; Villoresi, P. Stable, low-error, and calibration-free polarization encoder for free-space quantum communication. *Opt. Lett.* **2020**, *45*, 4706–4709. [CrossRef]
29. Agnesi, C.; Avesani, M.; Stanco, A.; Villoresi, P.; Vallone, G. All-fiber self-compensating polarization encoder for quantum key distribution. *Opt. Lett.* **2019**, *44*, 2398. [CrossRef]
30. Li, Y.-P.; Chen, W.; Wang, F.-X.; Yin, Z.-Q.; Zhang, L.; Liu, H.; Wang, S.; He, D.-Y.; Zhou, Z. Guo, G.-C.; et al. Experimental realization of a reference-frame-independent decoy BB84 quantum key distribution based on Sagnac interferometer. *Opt. Lett.* **2019**, *44*, 4523. [CrossRef]
31. Li, Y.; Li, Y.-H.; Xie, H.-B.; Li, Z.-P.; Jiang, X.; Cai, W.-Q.; Ren, J.-G.; Yin, J.; Liao, S.-K.; Peng, C.-Z. High-speed robust polarization modulation for quantum key distribution. *Opt. Lett.* **2019**, *44*, 5262. [CrossRef]
32. Ma, D.; Liu, X.; Huang, C.; Chen, H.; Lin, H.; Wei, K. Simple quantum key distribution using a stable transmitter-receiver scheme. *Opt. Lett.* **2021**, *46*, 2152. [CrossRef] [PubMed]
33. Ma, X.; Qi, B.; Zhao, Y.; Lo, H.-K. Practical decoy state for quantum key distribution. *Phys. Rev. A* **2005**, *72*, 0102326. [CrossRef]
34. Ding, Y.-Y.; Chen, W.; Chen, H.; Wang, C.; Wang, S.; Yin, Z.-Q.; Guo, G.-C.; Han, Z.-F. Polarization-basis tracking scheme for quantum key distribution using revealed sifted key bits. *Opt. Lett.* **2017**, *42*, 1023. [CrossRef]
35. Peng, C.-Z.; Zhang, J.; Yang, D.; Gao, W.-B.; Ma, H.-X.; Yin, H.; Zeng, H.-P.; Yang, T.; Wang, X.-B.; Pan, J.-W. Experimental long-distance decoy-state quantum key distribution based on polarization encoding. *Phys. Rev. Lett.* **2007**, *98*, 010505. [CrossRef]

Disclaimer/Publisher's Note: The statements, opinions and data contained in all publications are solely those of the individual author(s) and contributor(s) and not of MDPI and/or the editor(s). MDPI and/or the editor(s) disclaim responsibility for any injury to people or property resulting from any ideas, methods, instructions or products referred to in the content.